Large Eddy Simulation of the transient cavitating vortical flow in the wake of a hydrofoil

Jian Chen, Linlin Geng, Xavier Escaler[*]

Departament de Mecànica de Fluids, Universitat Politècnica de Catalunya - BarcelonaTech, Spain.

Abstract: The Zwart mixture cavitation model and the Large Eddy Simulation (LES) turbulence model have been combined to simulate the transient cavitating flow in the wake of a hydrofoil. The hydrofoil is a 2D NACA0009 with a truncated trailing edge which has been extensively investigated experimentally in the EPFL high-speed cavitation tunnel. The simulated flow conditions correspond to a free stream velocity of 20 m/s (Re = 2×10^6) and an incidence angle of $0°$ for different levels of cavitation number, σ, ranging from free cavitation to cavitation flow with different amounts of vapor. Under such hydrodynamic conditions and blunt trailing edge geometry, a Von Kármán vortex street takes place that is the object of the present study in order to ascertain how cavitation modifies the vortex structure and its dynamic behavior. The numerical results show a good agreement with the experimentally measured vortex shedding frequency without and with cavitation. As observed experimentally, the numerical results also predict an increase of the frequency induced by a significant change of the vortex properties. In order to identify the effects induced by the occurrence and development of cavitation, the obtained unsteady velocity field has been analyzed via Proper Orthogonal Decomposition (POD) technique to identify and understand changes in the flow structure. It has been found that the occurrence and development of cavitation can change the contribution of the POD modes to the total velocity filed. Moreover, the appearance of cavitation seems to stabilize the flow field unsteady behavior since high order POD modes are harmonically correlated with the first couple of basic POD modes.

Keywords: Von Kármán vortex shedding, cavitation, Proper Orthogonal Decomposition (POD).

1. Introduction

The phenomenon of vortex shedding behind the solid body, e.g., a wedge, a circular cylinder or a truncated hydrofoil, is commonly encountered in the field of hydraulic machinery and systems. As the local static pressure drops to the saturated vapor pressure, P_V, the inception of cavitation takes place. Thus, vaporous cavities are formed and develop inside the vortical coherent structures. In addition, the unsteady vortices dynamics, i.e., vortex shedding frequency and vortex formation length, tend to change significantly [1]. Furthermore, the occurrence of cavitation inside the rotational coherent structures is prone to systemically emphasize the noise, the vibrations and the cavitation erosion of hydraulic machinery [2-3].

In 1966, the cavitating vortex shedding phenomenon behind a 2D triangular wedge was firstly studied and reported by Young and Holl [4]. They found the fact that there is a dependence between the cavitation number and the Strouhal number. Also, their results show the existence of a maximum Strouhal number which may occur at half value of the incipient cavitation number. Later on, the observations of Young and Holl [4] were confirmed by Franc [5] and Ramamurthy et.al [6]. To explain the mechanism for the dependence between the cavitation number and the Strouhal number, Belahadji [1] investigated the rotational cavitation structures in a turbulent wake of a two-dimensional wedge. Thus, they found that the dynamics of the wake changes as soon as cavitation appears and that the variation of the distance between

two rows of primary vortices due the cavitation development may be responsible for the change of the Strouhal number. Unlike the two-dimensional wedge flow, the vortex shedding over the truncated hydrofoil NACA 0009 was investigated by Ausoni [7]. He found that, at high Reynolds numbers and low attack angles, the cavitating vortex shedding frequency increased monotonously with the cavitation number decrease. However, the mechanism inducing the variation of the vortices shedding frequency due to the development of cavitation has not been completely elucidated yet.

Thanks to the exponential development of CFD resources and tools, abundant works on vortical cavitation can be found in the literature. The latest great progresses have been made in the simulation of cavitation in vortical flows with Large Eddy Simulation LES [8-10]. These works have increased the understanding of the cavitation effects on the vortices/eddies dynamic behavior, ranging from the large scales to the intermediate ones. Besides, Gnanaskandan et al. [11] have used the LES turbulent model coupled with compressible homogenous cavitation model to further explore and ascertain the mechanism behind the cavitation effects on the vortex shedding frequency. More specifically, they argue that the variation of the Strouhal number with the development of cavitation is induced by the vorticity reduction due to the vorticity dilatation term. In conclusion, all of these researches show the advantage of LES turbulent modelling in the numerical simulation of cavitating vortical flow.

In this study, the Zwart mixture cavitation model coupled with the LES wall-adapting local eddy-viscosity turbulence model has been used to simulate the cavitating vortex shedding flow over the truncated hydrofoil NACA 0009 at three different cavitation numbers, ranging from a cavitation free regime to a well-developed cavitation flow. Based on these numerical results, the present objectives of this study has been to assess the effects induced by the development of cavitation in the turbulent wake flow. To explore the cavitation effects in details, the Proper Orthogonal Decomposition (POD) method [12] has been applied the velocity field in the wake obtained from the numerical results. Then, the obtained modes between the different regimes have been compared and the alterations induced by the development of cavitation have been identified, which may help to understand the mechanisms behind the increase of the vortex shedding frequency with the reduction of the cavitation number.

2. Numerical methods

The experimental tests taken as a reference to validate our numerical models and results were carried out at the EPFL high-speed cavitation tunnel with a NACA 0009 hydrofoil inside a rectangular test section of dimensions 150×150×750 mm³. The hydrofoil chord length, C, and the span, SP, were 100 and 150mm, respectively. For additional details, see Ausoni's thesis [7]. Based on these dimensions, the corresponding two-dimensional computational domain and the generated mesh with details of the near wake region are shown in Figure 1.
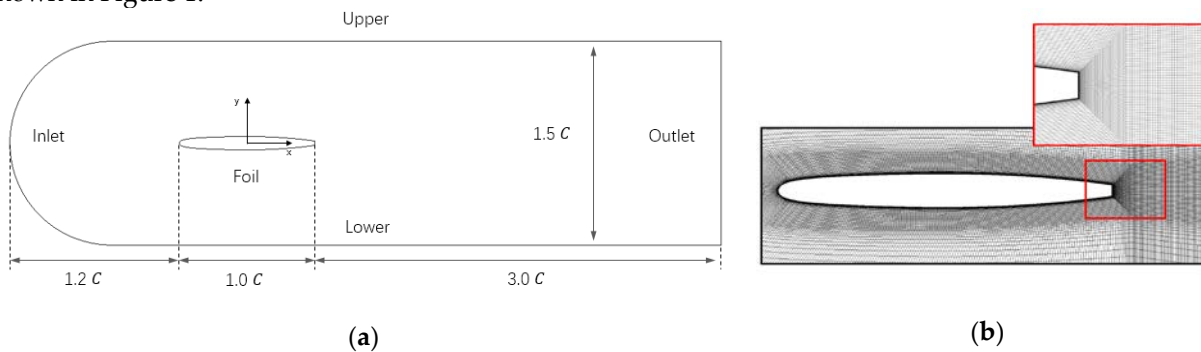

(a)   (b)

Figure 1. Computational domain geometry of the hydrofoil in the test section (a), and mesh topology at the vicinity of hydrofoil surface and the trailing edge in the near wake region (b).

To simulate a cavitation flow, the most commonly used physical models are based on the homogenous mixture model, e.g. Kunz et al. [13], Zwart et al. [14], and Schnerr et al. [15]. Among them, the Zwart cavitation has been selected in present study for its simplicity and robustness. Meanwhile, the LES wall-adapting local eddy-viscosity turbulence model has also ben adopted in the numerical simulations. For the boundary conditions, a uniform inflow at 20 m/s was set at the inlet. Moreover, a constant pressure was applied at the outlet boundary based on the corresponding cavitation number, $\sigma = \frac{p_\infty - p_v}{1/2 \rho V_{inlet}^2}$, where p_∞ is the reference pressure, which is set to equal the pressure located at the outlet boundary. The cavitation number range, σ/σ_i, has been taken from 1.3 to 0.4, where σ_i corresponds to the inception cavitation number.

POD is one of the most popular methods to obtain the modal decomposition of a flow property. With this method, a set of instantaneous data, $x_1, \ldots, x_m \in \mathbb{R}^n$, are re-arranged and form a new matrix X, whose j^{th} columns are the snapshot vector x_j. Then, the singular value decomposition is applied to the matrix X to obtain:

$$X = U\Sigma V^T = \sum_{j=1}^{r} \sigma_j u_j v_j^T \tag{1}$$

where, r is the matrix rank of X, U is the $n \times r$ matrix with orthonormal columns vector u_j, Σ is $r \times r$ diagonal matrix and V is the $m \times r$ matrix whose columns v_j are orthonormal to each other. Here, the vector of columns u_j are the POD modes of matrix X. To obtain the time coefficient $a_j(t)$, the instantaneous data matrix X are projected on the r rank subspace with basis vector u_j:

$$A = \sum_{j=1}^{r} a_j(t) u_j^T \tag{2}$$

where A is the time coefficient of the POD modes, and $a_j(t)$ is the columns vector of A.

3. Results

3.1. Validation of numerical results

To validate the unsteady results predicted by the numerical simulation of the vortex shedding dynamic behavior, a Fast Fourier transform (FFT) has been applied to the time history of the lift coefficient, $C_L = \frac{F_L}{1/2 \rho V_{inlet}^2 A_{ref}}$, where F_L is the vertical force acting on the hydrofoil, ρ is the water density, and A_{ref} is the reference area. Compared with the experimental Strouhal values, $St = \frac{fh}{V_{inlet}}$ where h denotes the height of the trailing edge, the present numerical results show a relatively good agreement (Figure 2). Moreover, the increasing trend of the vortex shedding frequency with the reduction of the cavitation number is also very well captured.
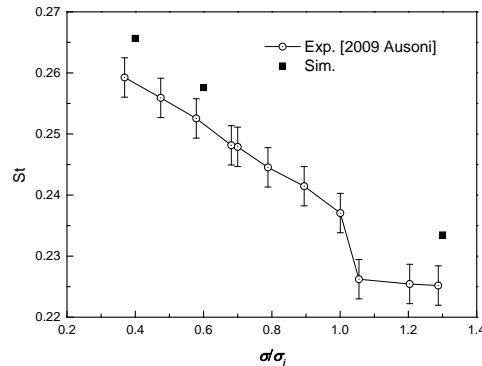

Figure 2. Comparison between numerical and experimental St values.

3.2. POD post-processing

The POD method has been applied to the instantaneous wake velocity field, $V(\boldsymbol{u}, \boldsymbol{v})$, where $\boldsymbol{u}$ and $\boldsymbol{v}$ denote the horizontal (stream wise) and vertical (perpendicular to the flow) components of the velocities, which are obtained from the numerical simulations of the cavitating vortex shedding flow in vicinity of the rear part of the hydrofoil at different cavitation numbers. More specifically, 1001 instantaneous vectors, $\boldsymbol{x}_j = (\boldsymbol{u}(\boldsymbol{x}_1, \boldsymbol{y}_1, \boldsymbol{t}_0), \dots, \boldsymbol{u}(\boldsymbol{x}_i, \boldsymbol{y}_j, \boldsymbol{t}_{1000}), \boldsymbol{v}(\boldsymbol{x}_1, \boldsymbol{y}_1, \boldsymbol{t}_0), \dots, \boldsymbol{v}(\boldsymbol{x}_i, \boldsymbol{y}_j, \boldsymbol{t}_{1000}))$, form the matrix $\boldsymbol{X}$.

The first 5 POD modes are considered to represent the main contribution to the velocity field, according to the equation $\lambda_i / \sum \lambda_i$, where the λ_i is the ith diagonal element of matrix $\boldsymbol{\Sigma}$ in Equation (1). Therefore, in Figure 3 they are plotted for the horizontal (stream wise) velocity component field at the three flow conditions corresponding to no cavitation and cavitation. Two noticeable observations can be obtained from the comparison between the basic POD modes at different cavitation numbers. Firstly, it is observed from the first POD modes that the transient region near the trailing edge of the hydrofoil increases in stream wise length as cavitation increases. Moreover, it is also found that the horizontal spacing between the centers of the observed cells is reduced as cavitation develops. Secondly, the contribution of the two lowest POD modes (1) tends to increase from no cavitation (with a 32.3%) to well-developed cavitation (with a 41.7%). Furthermore, the first 5 modes contribute with a 74.5% for the no cavitation regime, meanwhile when cavitation occurs and develops, the contribution of first 5 modes increases to 80.6% at $\sigma/\sigma_i = 0.6$ and to 89.8% at $\sigma/\sigma_i = 0.4$.
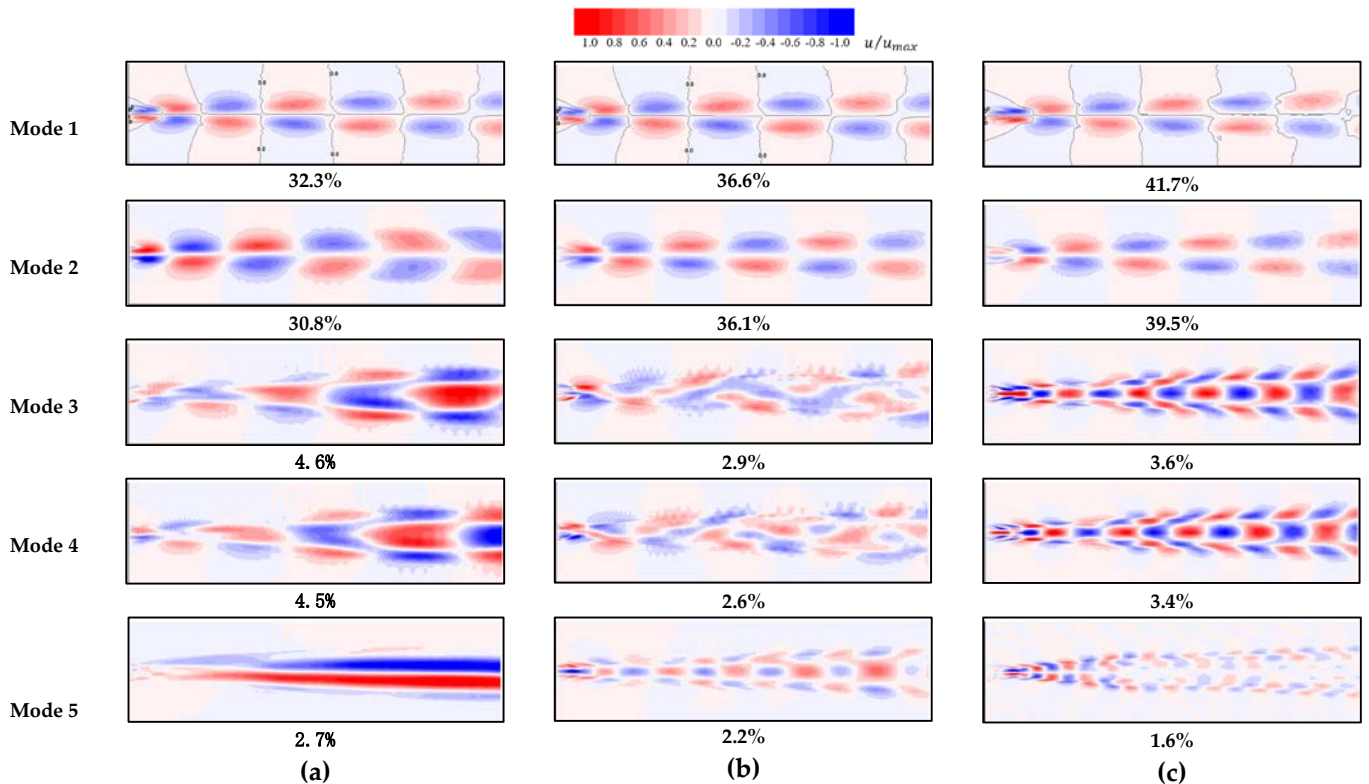

Figure 3. POD mode decomposition of the horizontal (stream wise) flow field, **u**, and their percent contribution to the total velocity field for modes 1 to 5 at different cavitation numbers: (a) $\sigma/\sigma_i = 1.3$, (b) $\sigma/\sigma_i = 0.6$ and (c) $\sigma/\sigma_i = 0.4$.

The orbits of the POD time coefficients, $a_j(t)$, have been compared for different cavitation numbers. Figure 4 shows the orbit plots of the modes 2 to 6 time coefficients, $a_j(t), j = 2,..,6$, as a function of the mode 1 time coefficients, $a_1(t)$. From these plots it can be seen that all the shapes found with $a_2(t)$ as a function of $a_1(t)$ illustrate a periodic phenomenon, even for different cavitation numbers. Since this phenomenon is repeated and maintained, it suggests that the first couple of POD modes (1 and 2) are the basic modes representing the vortical flow structures. However, as cavitation develops, it can be see that the orbits of the high order POD modes as a function of $a_1(t)$ become more regular, which suggests that these higher order modes become more coherent and a multiple or harmonic of the first POD mode when cavitation forms within the cores of the vortices.
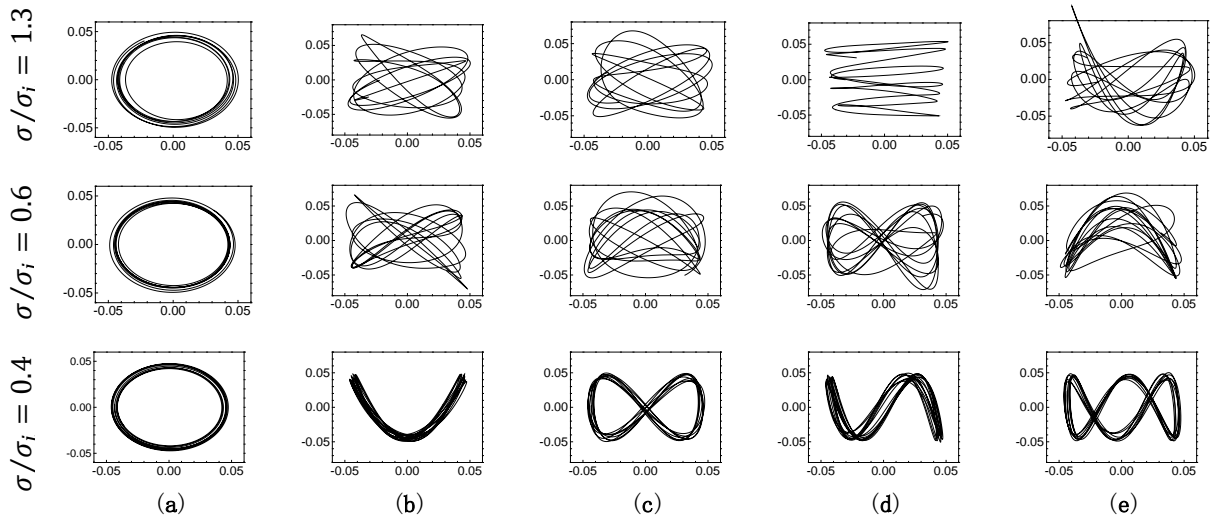

Figure 4. Orbits of the POD time coefficients for modes 2 to 6 as function of mode 1 at different cavitation conditions.(a) $a_2(t)$ vs $a_1(t)$; (b) $a_3(t)$ vs $a_1(t)$; (c) $a_4(t)$ vs $a_1(t)$; (d) $a_5(t)$ vs $a_1(t)$; (e) $a_6(t)$ vs $a_1(t)$.

4. Conclusions

The dynamic characteristics of the cavitating wake flow behind a 2D NACA0009 with a blunt trailing edge have been numerically investigated. For that, the obtained velocity fields at different cavitation numbers have been decomposed by the POD method. It has been found that the occurrence and development of cavitation indeed affects the basic modes of the vortex shedding process in the vicinity of the truncated trailing edge. Firstly, the cavitation tends to enlarge the vortex formation region and to reduce the spacing between the cells corresponding to the basic velocity modes. Secondly, the contribution of the lowest POD modes tends to increase with the decrease of cavitation number. Finally, stronger coherences are found between the time coefficients of the higher order modes and the ones of mode 1 with the development of cavitation. In summary, these observations are in agreement with the experimental observations showing an increase of the shedding frequency and of the coherence of the vortical structures when cavitation takes place.

References

1. Belahadji, B.; Franc, J.P.; Michel, J.M. Cavitation in the rotational structures of a turbulent wake. *J. Fluid Mech.* **1995**, *287*, 383–403.

2. Arndt, R.E. Cavitation in fluid machinery and hydraulic structures. *Annu. Rev. Fluid Mech.* **1981**, *13*, 273–326.

3. Franc, J.P.; Michel, J.M. *Fundamentals of Cavitation*; Springer science & Business media: Berlin, Germany, 2006; pp. 1–13,247–262.

4. Young, J.O.; Holl, J.W. Effects of cavitation on periodic wakes behind symmetric wedges. *J. Fluids Eng.* **1966**, *88*, 163–176.

5. Franc, J. P.; Michel, J. M. ; Lesieur, M. Structures rotationnelles bi et tri-dimensionnellesdans un sillage cavitant. *C.R. Acad. Sci.* **1982,** *295*, 773-777.

6. Ramamurthy, A.S.; Balachandar, R. Characteristics of constrained cavitating bluff body wakes. *J. Eng. Mech.* **1991**, *117*, 513–531.

7. Ausoni, P. Turbulent Vortex Shedding from a Blunt Trailing Edge Hydrofoil. Ph.D. Thesis, EPFL, Lausanne, Switzerland, 2009.

8. Trummler, T.; Schmidt, S.J.; Adams, N.A. Investigation of condensation shocks and re-entrant jet dynamics in a cavitating nozzle flow by Large-Eddy Simulation. *Int. J. Multiph. Flow* **2020**, *1*, 215–241.

9. Asnaghi, A.; Svennberg, U.; Bensow, R.E. Large Eddy Simulations of cavitating tip vortex flows. *Ocean. Eng.* **2020**, *195*, 106–133.

10. Budich, B.; Schmidt, S.J.; Adams, N.A. Numerical simulation and analysis of condensation shocks in cavitating flow. *J. Fluid Mech.* **2018**, *10*, 759–791.

11. Gnanaskandan, A.; Mahesh, K. Numerical investigation of near-wake characteristics of cavitating flow over a circular cylinder. *J. Fluid Mech.* **2016**, *790*, 453-491.

12. Berkooz, G.; Holmes, P.; Lumley, J.L. The proper orthogonal decomposition in the analysis of turbulent flows. *Annu. Rev. Fluid Mech.* **1993**, *25(1)*, 539-575.

13. Kunz, R.F. ; Boger, D.A. ; Stinebring, D.R. A preconditioned Navier-Stokes method for two phase flows with application to cavitation prediction. *Comput. Fluids.* **2000**, *29*, 849–875 .

14. Zwart, P.J. ; Gerber, A.G. ; Belamri, T. A two-phase flow model for predicting cavitation dynamics. In: Proceedings of the Fifth International Conference on Multiphase Flow, Yokohama, Japan, 2004.

15. Schnerr, G.H.; Sezal, I.H.; Schmidt, S.J. Numerical investigation of three-dimensional cloud cavitation with special emphasis on collapse induced shock wave dynamics. *Phys. Fluids.* **2008**. *20*, 040703